Evidence for Gap Flows in the Birch Creek Valley, Idaho

D. FINN AND B. REESE

Field Research Division, NOAA/Air Resources Laboratory, Idaho Falls, Idaho

B. BUTLER AND N. WAGENBRENNER

Fire Sciences Laboratory, U.S. Forest Service, Missoula, Montana

K. L. CLAWSON AND J. RICH

Field Research Division, NOAA/Air Resources Laboratory, Idaho Falls, Idaho

E. RUSSELL, Z. GAO, AND H. LIU

Laboratory for Atmospheric Research, Washington State University, Pullman, Washington

(Manuscript received 10 February 2016, in final form 25 August 2016)

ABSTRACT

A field study was conducted of flows in the Birch Creek Valley in eastern Idaho. There is a distinct topographic constriction in the Birch Creek Valley that creates two subbasins: an upper and lower valley. The data were classified into one of three groups based on synoptic influence (weak/absent, high wind speeds, and other evidence of synoptic influence). Gap flows commonly developed downwind of the constriction in association with the weak/absent group but also occurred in association with the two synoptic groups suggesting the potential for more diverse origins. In general, the frequency and strength of gap flows appeared to be linked to the development of the requisite thermal regime and minimization of any synoptically driven southerly winds that would suppress outflows. Gap flows were characterized by high wind speeds with jetlike vertical profiles along the axis of the lower valley. For all three groups the morning transition in the upper valley and western sidewall usually proceeded slightly ahead of the lower valley, consistent with the principles of the topographic amplification factor. The persistence of southerly winds in the lower valley past evening transition inhibited the development of gap flows, promoted strong nighttime inversions, and delayed the onset of morning transition relative to the upper valley. Nocturnal temperature inversions in the lower valley were largely eliminated with the onset of strong gap flows resulting in earlier morning transitions there. The form for a method of predicting gap flow wind speeds is proposed.

1. Introduction

Strong nocturnal downvalley, low-level exit jets are often associated with narrow, constricted valleys. They have been identified in many parts of the world (Zardi and Whiteman 2012) including numerous Alpine valleys (e.g., Muller et al. 1984; Pamperin and Stilke 1985; Zängl 2004; Mayr et al. 2004, 2007), in interior mountainous areas of the American West (e.g., Banta et al. 1995; Stewart et al. 2002; Darby et al. 2006; Chrust et al. 2013), the Columbia River gorge (Sharp and Mass 2002, 2004), and in Iran (Liu et al. 2000). They have often been identified in conjunction with a topographic constriction that results in what are termed gap flows.

Gap flows have been defined as "an asymmetric flow through a topographical constriction (lateral and/or vertical) driven by different 'reservoirs' of air on either side of the gap, with a deeper slowly moving layer upstream of the gap and a thinner much faster layer downwind of the gap" (Mayr et al. 2007, p. 881). They arise as a result of a pressure gradient between two air masses separated by an intervening constriction. The pressure gradient can be large scale and due to synoptic factors and/or smaller scale and thermally driven. In mountainous terrain, the latter results in nocturnal downvalley jets in fair weather conditions.

Corresponding author address: D. Finn, NOAA/Air Resources Laboratory, Field Research Division, 1750 Foote Dr., Idaho Falls, ID 83402.
E-mail: dennis.finn@noaa.gov

DOI: 10.1175/JAS-D-16-0052.1

Several features of gap flows have been identified. The maximum wind speeds are usually not found in the constricted volume of the gap but instead in the exit region where there is an acceleration beyond the gap due to the along-valley pressure gradient (Sharp and Mass 2002, 2004; Mayr et al. 2007; Chrust et al. 2013; Overland and Walter 1981; Bendall 1982; Dorman et al. 1995; Colle and Mass 2000). The wind speeds associated with a jet exiting a gap can actually reach a maximum several kilometers downwind of the gap (Zängl 2004; Sladkovic and Kanter 1977; Pamperin and Stilke 1985). Upwind of the gap, winds are light in a deep flow layer with wind speed maxima elevated well above the surface in contrast to a much shallower layer with low-level wind speed maxima downwind of the gap (Zängl 2004; Chrust et al. 2013). Nocturnal wind speeds upwind of the constriction are much lower than downwind of the constriction.

Despite the extensive studies of winds in mountain–valley terrain (Whiteman 1990; Zardi and Whiteman 2012; Fernando et al. 2016), there are some features of gap flows that are not fully understood. Most studies of diurnal mountain wind systems have focused on fair weather, anticyclonic conditions when thermal forcing is the dominant factor (Zardi and Whiteman 2012). Gap flow behavior under synoptic conditions in mountain wind systems is less well known. It is also the case that valleys with ostensibly similar settings or configurations might exhibit strong gap flows, weak gap flows, or none at all. The along-valley behavior of the jet through and downwind of a gap is much better documented than the lateral spread behavior of the jet (Zängl 2004; Chrust et al. 2013). Furthermore, it has been emphasized that every site offers a topographic configuration or combination of other factors (e.g., vegetative cover, slope aspect, soil moisture) that can affect the patterns and timing of complex flows and that additional study continues to enhance our understanding of the potential variability (Zardi and Whiteman 2012).

The topographic amplification factor (TAF) is considered to be a basic thermodynamic factor that drives the mountain–valley wind system (Steinacker 1984; Whiteman 1990; Schmidli 2013) although TAF is sometimes an oversimplification owing to the potential for heat exchange outside the valley (Rampanelli et al. 2004; Schmidli and Rotunno 2012; Schmidli 2013; Zardi and Whiteman 2012). The basis for the idea lies in the observation that diurnal temperature amplitudes in mountain valleys are much larger than over adjacent plains. The valley has a smaller volume of air than the adjoining plain. Smaller volumes of air require less energy gain/loss to heat/cool more quickly than larger volumes of air. The TAF describes how the differential heating/cooling sets up horizontal temperature differences between the valley and plain that result in a pressure gradient that drives the flow.

The American West comprises a very large and complex assemblage of mountains, mountain valleys, intermontane basins, and plains with total vertical relief commonly in excess of 1 km—often much more. Therefore, it presents the potential for observing significant variation in complex mountain–valley wind behavior. The Birch Creek Valley (BCV) is a large valley in eastern Idaho that offers much of this variety. Three groups collaborated on the BCV project: the Air Resources Laboratory Field Research Division (ARLFRD) of NOAA, the U.S. Forest Service Fire Sciences Laboratory (FSL), and the Laboratory for Atmospheric Research (LAR) at Washington State University. The FSL was seeking to acquire additional datasets to improve the modeling and prediction of wildfire behavior in complex terrain (Forthofer et al. 2014; Butler et al. 2015).

Analysis of the project database after completion of the field measurements revealed the presence of nighttime and early morning gap flows in the BCV under certain conditions. The principal focus of the analysis will be on these gap flows. This will include their origin, evolution, frequency, and strength relative to synoptic influences and the role of atmospheric stability. Initial attention will be directed to quiescent, fair weather conditions but then expand to evaluate the effects of a broader range of synoptic conditions. Secondarily, the role of TAF and gap flows on the timing of morning transition will be examined.

There are important reasons for understanding gap flows in the American West. Perhaps most important is the need to accurately model and predict wildfire behavior as the fire season grows longer and the number and intensity of fires in the American West increases (e.g., Westerling et al. 2006; Flannigan et al. 2009). The need for understanding these phenomena with respect to wildfires is clear given that 1) many wildfires occur in mountainous, complex terrain, and 2) there is some potential for the presence of gap flows to influence wildfire behavior in many situations. Improved understanding of gap flow behavior could be helpful in any situation where gap flows might be a factor.

2. Site description, measurements, and methodology

a. Site description

The BCV field study area is shown in Fig. 1 as a major, steep-sided intermontane valley that intersects the Snake River Plain (SRP). The NNW-trending BCV is about 60 km long and ranges from about 19 to 24 km wide between the crests of the Lemhi Range to the west

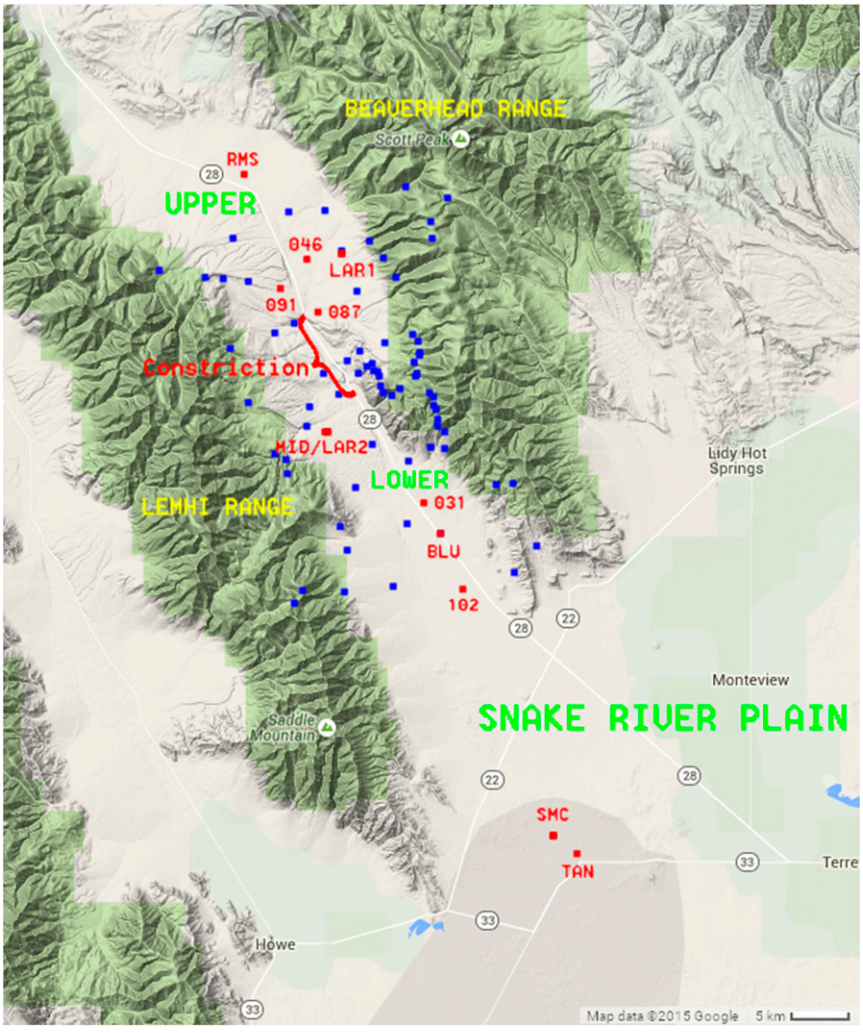

FIG. 1. Birch Creek Valley field study map showing locations of key ARLFRD, LAR, and FSL sites referenced in the text (red) and other FSL sites (blue). The FSL sites are identified by a three-digit number.

and Beaverhead Range to the east. It is separated by a low pass on its north end from the NNW-trending intermontane valley containing the northward-flowing Lemhi River. In cross section, BCV is asymmetric with greater relief to the west. The maximum vertical relief with respect to the surrounding mountains is about 1500 m and there are significant topographical variations across the floor of the valley itself. Prominent among these are a complex of alluvial fans shed from the Lemhi Range. These deposits have been scored by numerous small drainages flowing from west to east. The total relief across the fans from the base of the Lemhi Range to Birch Creek along the axis of the valley is up to 300–350 m. On the eastern side of the valley there is a prominent promontory of the Beaverhead Range extending into BCV. The alluvial fans from the west abut against the outcroppings to the east, in effect, dividing BCV into an upper and lower valley. Birch Creek breeches these cross-valley obstructions through a pair of narrow, shallow constrictions near where the alluvial fans meet the eastern outcrops (Fig. 1). The alluvial fans in Fig. 1 are visible as the finely etched gray surfaces to the west and northwest of the constriction. Except for the eastern promontory, the cross-valley obstructions form more of a sloped, irregular, corrugated complex than they do a high barrier. However, the overall physical effect is the formation of two air masses with dissimilar flow regimes in the upper and lower valleys during certain meteorological conditions. These differences are highlighted in the analyses below.

The area is generally arid and dominated by sagebrush steppe. Some forested areas are present, mainly in limited areas on north and east facing slopes along the eastern flank of the Lemhi Range. Sensible heat flux was

dominant over latent heat flux during the experimental period (Russell et al. 2015).

b. Measurements

An extensive suite of meteorological measurements was made during the period selected for data analysis (13 June to 6 September 2013; Julian days 164–249). The location of these measurements is shown on Fig. 1. Times stated in the text are mountain standard time (MST). For the given period of study, sunrise at nearby Idaho Falls on the SRP varied from 0430 to 0545 h. Sunset varied from 2015 to 1900 h.

1) CUP ANEMOMETERS AND WIND VANES, FSL

The FSL deployed 75 cup anemometers and wind vanes. Most were arrayed on a regular grid across the upper and lower valley with an enhanced density of sampling in the most rugged terrain at the edge of the mountains on both the east and west sides. Measurements were made at 1 Hz at a height of 3.0 m AGL and the wind speed U and wind direction data were averaged and recorded at 30-s intervals. The record for many of the anemometers is incomplete and there was a gradual attrition with time due to instrument problems (e.g., cattle knocking them over, etc.).

2) SONIC ANEMOMETERS, ARLFRD

ARLFRD deployed four R.M. Young 81000 Ultrasonic anemometers at 3.2 m AGL at the RMS, MID, BLU, and TAN sites (Fig. 1). Data were archived at 10 Hz using an Acumen datalogger. The RMS site was on the east side in the upper valley on gently sloped terrain. MID was located along the western sidewall of the lower valley, on a slope with an average grade of about 5%, a short distance south of the cross-valley complex. Its location provided exposure to the early morning sun. BLU is a NOAA/INL Mesonet site located on very gently sloped terrain on the valley floor approximately midway between the cross-valley complex and the transition from the BCV to the SRP near the axis of the BCV. TAN and SMC are located on the INL about 11 km outside BCV on the SRP in alignment with the axis of BCV. Two-axis rotation into the mean wind (Aubinet et al. 2000) was applied to the sonic anemometer data.

3) FLUX STATIONS, LAR

LAR deployed two flux stations. Four CSAT-3 sonic anemometers from Campbell Scientific were deployed at 3 and 8 m AGL on towers at LAR1 (upper valley) and LAR2 (lower valley, near MID). Data were archived at 10 Hz. Temperature measurements were made at the 3- and 8-m levels using Campbell Scientific HC2S3 and HMP45C sensors at the LAR1 and LAR2 sites, respectively. The LAR1 temperature measurements were only available for Julian days 176 to 197.

4) SODAR

Three sonic detection and ranging (sodar) devices were deployed during the field study by ARLFRD. An Atmospheric Research Technologies (ART) sodar was deployed at the MID site. Atmospheric Sciences Corporation (ASC) sodars were deployed at BLU and TAN. The sodars measured 10-min-average wind speed and direction profiles from 30 up to 200 m AGL, depending on the data recovery. For the sake of brevity, data from the TAN sodar will not be presented. An additional ART sodar was deployed at RMS by FSL but the record has numerous gaps owing to power supply problems and is not included in this analysis. Hourly averages of the 10-min averages will be shown.

5) RADAR PROFILER

A LAP-3000 radar profiler operating at 924 MHz was deployed at BLU by ARLFRD. The profiler measured wind speed and direction profiles at 28 levels beginning at 151 m AGL up to 2746 m at approximately 100-m increments. Like the sodars, the data recovery height varied in response to atmospheric conditions. Half-hour averages were recorded and hourly averages were calculated from these averages.

6) NOAA/INL MESONET

ARLFRD maintains a network of 34 meteorological stations across eastern Idaho with emphasis on the INL (Clawson et al. 2007). Data from two of these stations were utilized in this analysis by aggregating 5-min-average data to 10-min averages. The SMC site is located on the SRP, at the north end of the INL near TAN, and is often affected by outflows from BCV. It uses cup anemometers and wind vanes to measure wind speed and direction at 2, 10, 15, and 45 m AGL. Temperatures are measured at the 2-m height using a Vaisala HMP45C and differential thermocouple at the other heights. Other measurements include relative humidity at 2 m and incoming solar radiation and precipitation. The BLU site is located within the lower BCV and winds there are highly influenced by its location. Measurements include cup anemometer and wind vane at 15 m AGL, temperatures at 2 and 15 m AGL, incoming solar radiation, and precipitation.

c. Methodology

The SMC mesonet site lies at the northern end of the INL and the 10-m daytime winds there were used as a reference for classification of days into the three groups.

TABLE 1. Summary of group classification criteria.

THRM	No sustained periods of daytime southwesterly winds at SMC at 10 m with $U > 7\,\mathrm{m\,s^{-1}}$ and no precipitation, little or no solar attenuation, and the absence of abrupt fluctuations in the time series of wind speed, wind direction, and/or virtual temperature at the sonic anemometers within BCV.
SYNW	Sustained periods of daytime southwesterly winds at SMC at 10 m with U mainly $> 7\,\mathrm{m\,s^{-1}}$ but with no precipitation, minimal solar attenuation, and minimal or absent abrupt fluctuations in the time series of wind speed, wind direction, and/or virtual temperature at the sonic anemometers within BCV.
SYNX	Days with measurable precipitation and/or significant solar attenuation and/or significant abrupt fluctuations in the time series of wind speed, wind direction, and/or virtual temperature at the sonic anemometers within BCV. At SMC U could be greater or less than $7\,\mathrm{m\,s^{-1}}$.

Sustained southwesterly winds are common during the summer months on the INL, especially during the afternoon (Clawson et al. 2007). In the absence of synoptic forcing, the southwesterly winds are thermally driven and wind speeds are light to moderate. Under the influence of synoptic forcing, the southwesterly winds are strong during the afternoon. Winds can be strong at SMC at other times of day as well but these are generally associated with nighttime northwesterly winds that can affect the northern parts of the INL. They are usually the result of nonsynoptic, thermally driven outflows from BCV and adjacent valleys but are occasionally due to a frontal passage.

The 86 days from 13 June to 6 September 2013 were classified into one of three groups based upon a combination of factors and a diurnal day from 0800 to 0800 h MST (Table 1). This breakdown was used because solar heating in nonsynoptic conditions drives the evolution of thermally dominated winds during the day and sets the stage for winds overnight until the following

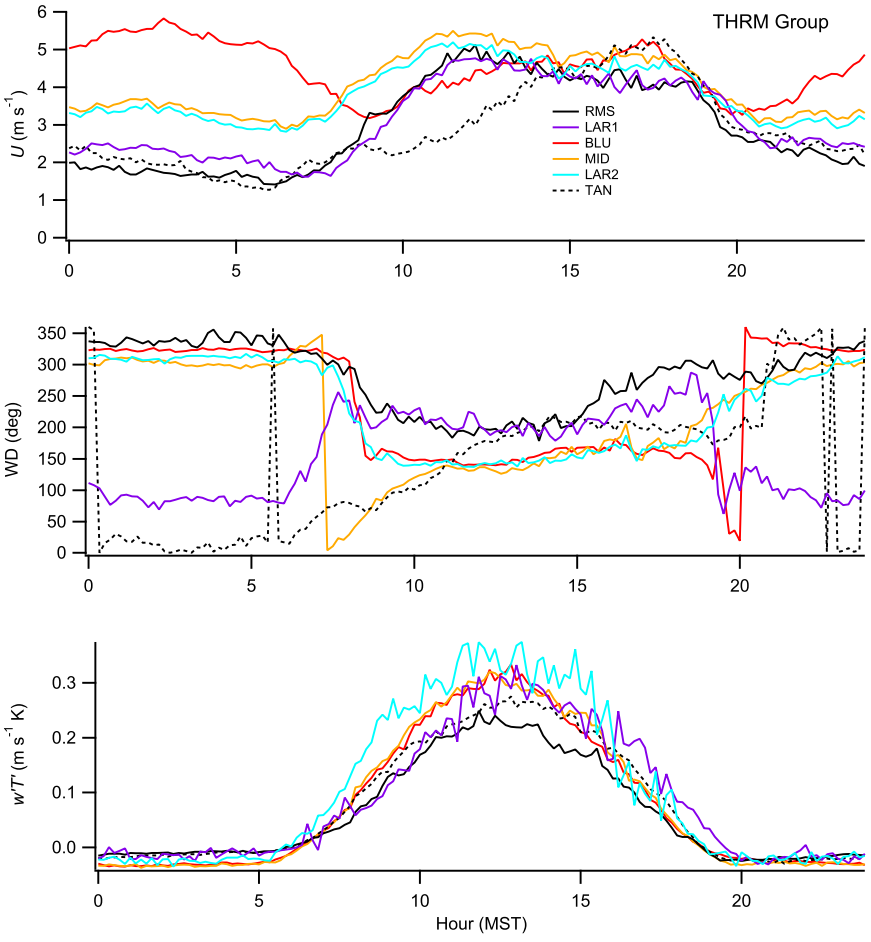

FIG. 2. Diurnal time series using 10-min averages of wind speed U, wind direction, and sensible heat flux $\langle w'T' \rangle$ at sonic anemometers for all THRM group days.

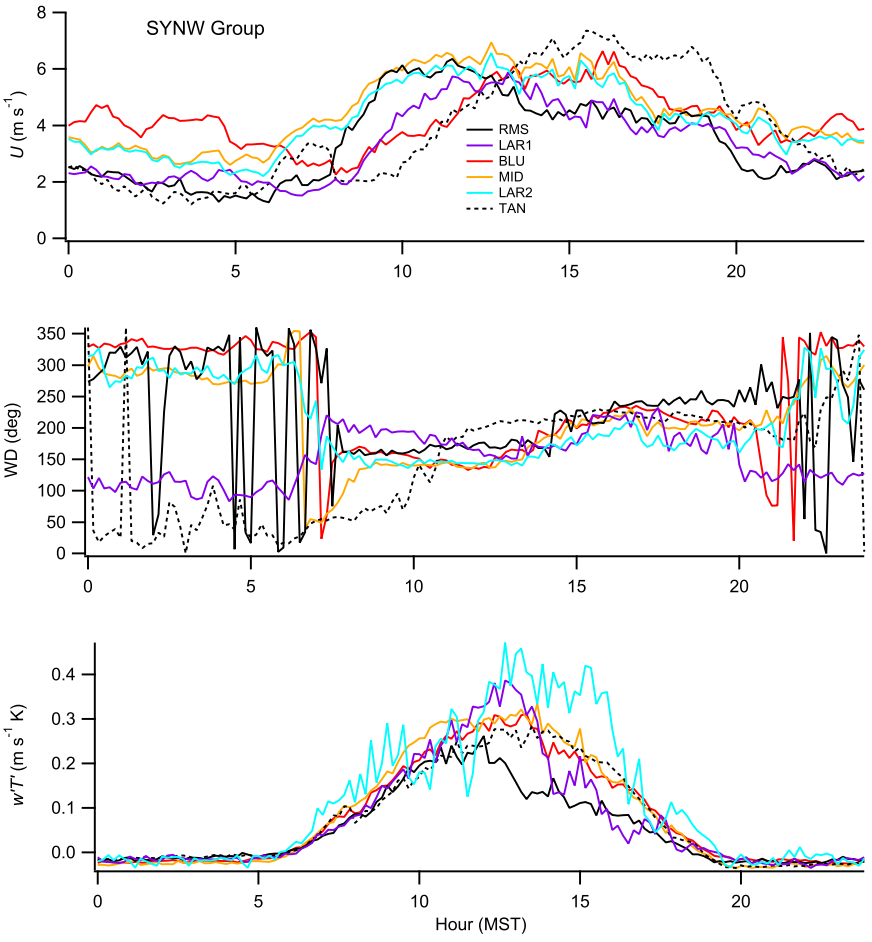

FIG. 3. As in Fig. 2, but for all SYNW group days.

morning. The THRM group was designated for days where winds were dominantly affected by a thermal regime without synoptic influence. The SYNW group was designated for days that were significantly affected by synoptic influences, primarily expressed as sustained strong daytime winds in the absence of other evidence for synoptic influences. The SYNX group was designated for those days that exhibited other evidence of disruption to a dominantly thermally driven regime, with or without high wind speeds. THRM, SYNW, and SYNX were assigned 44, 16, and 26 days, respectively.

The classification factors included wind speed and direction at SMC, precipitation and solar radiation records at the BLU and SMC mesonet sites, and the time series of wind speed, wind direction, and virtual temperature at the sonic anemometers within BCV. A day was excluded from THRM for any of the following conditions:

- periods with sustained high daytime wind speeds at SMC $> 7\,\mathrm{m\,s^{-1}}$,
- any measured precipitation,
- any significant attenuation of the daily solar radiation, or
- any abrupt fluctuation in the time series of wind speed, wind direction, or virtual temperature that suggested the occurrence of a weather event that could have disrupted wind patterns associated with the thermal regime (e.g., gust front from thunderstorm activity).

The mean 10-m wind speeds at SMC from 0900 to 1600 h MST for all THRM, SYNW, and SYNX group days were 3.55 ± 1.85, 5.43 ± 3.17, and $4.36 \pm 3.03\,\mathrm{m\,s^{-1}}$, respectively.

The THRM days were further subdivided into two groups based primarily on the 15 m U and the difference in temperature between the 2- and 15-m levels at BLU ($\Delta T = T_{\mathrm{top}} - T_{\mathrm{bottom}}$). GAP (strong gap flow) cases are defined as sustained $U > 8\,\mathrm{m\,s^{-1}}$ with $\Delta T < 2$°C at BLU after midnight and with light winds in the upper valley. INV (for strong inversion) cases are defined as $\Delta T >$ 4°C at some time at night after 2200 h with $U < 4\,\mathrm{m\,s^{-1}}$ at BLU. It took until at least 2200 h to achieve sustained periods with $\Delta T > 4$°C. The GAP and INV

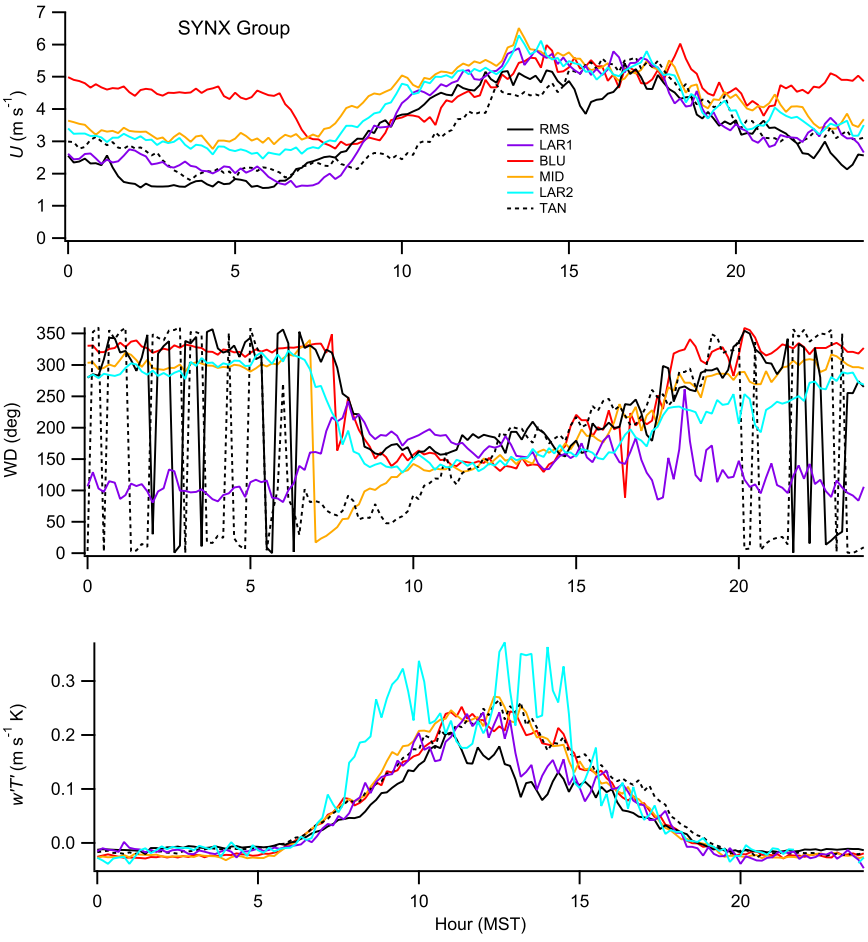

FIG. 4. As in Fig. 2, but for all SYNX group days.

subpopulations of THRM had mean daytime SMC wind speeds of 3.47 ± 1.73 and 3.58 ± 1.78 m s^{-1}, respectively.

Atmospheric stability data will be shown using the Brunt–Väisälä frequency N. There were significant gaps in the temperature record at LAR1. While there were also some gaps in the sonic anemometer record at LAR1, it was more complete, so the virtual temperatures from those measurements at 3 and 8 m AGL were used in calculating N at that station. While still incomplete, this enabled an expansion of the analysis to include more days from the upper valley. The sonic anemometer measurements were also used at LAR2. The calculations at BLU and SMC utilized the temperature measurements at 2 and 15 m AGL. Of the 44 THRM days, 23 were assigned to GAP and 8 were assigned to INV. The morning transition will be defined in terms of the shift in wind direction from downvalley to upvalley, the increase in wind speed following the early morning minimum, and a change from negative to positive sensible heat flux. There was local variability in sunrise and sunset across the study area owing to the large topographic relief of the bounding mountains, relative to the times stated in section 2b. The averages shown in section 3 were calculated at the sites identified for each time period, within each data classification, and incorporate some variability with respect to sunrise and sunset.

3. Results

a. Anemometers

The ARLFRD and LAR sonic anemometer results are summarized in Figs. 2–4 for all THRM, SYNW, and SYNX group days, respectively. The most striking feature of the wind speed data was the distinction between stations located in the lower valley (BLU, MID, LAR2) and those located in the upper valley (RMS, LAR1) or out on the plain (TAN). First, the average nocturnal wind speeds at BLU, MID, and LAR2 were much higher than at RMS and LAR1, especially for THRM. These higher nocturnal wind speeds in the lower valley were associated with northwesterly, downvalley gap flows.

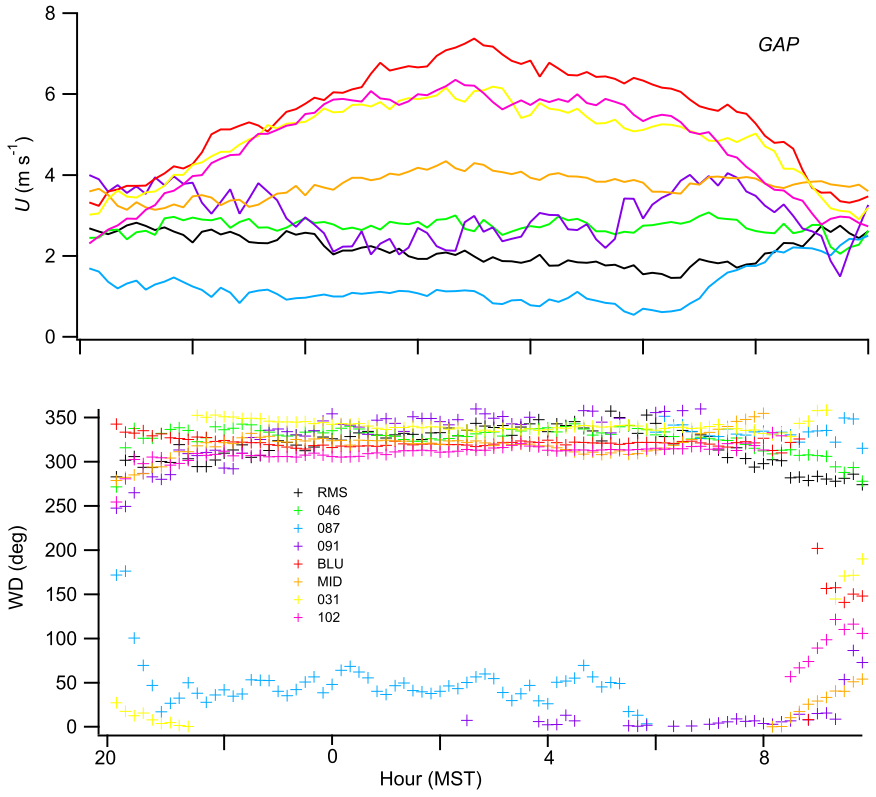

FIG. 5. Wind speed and direction in the upper (RMS, 046, 087, 091) and lower (BLU, MID, 031, 102) valleys for all days in THRM GAP from 2000 to 1000 h.

The nighttime easterly winds at LAR1 might have been due to outflows from a small side canyon in the Beaverhead Range to the east and/or downslope flows due its location east of the axis of the valley. The nighttime northeasterly winds at TAN were associated with a prevalent regional drainage flow on the SRP.

There was also a distinction in the diurnal trends in sensible heat flux when THRM is compared to SYNW and SYNX. Both SYNW and SYNX exhibited an afternoon attenuation of sensible heat flux in the upper valley compared to the lower valley that is not apparent in THRM. Presumably this was linked to increased afternoon cloudiness.

A close examination also reveals a 1- to 2-h delay in the increase of U in the morning at BLU relative to the sidewall (MID, LAR2) and upper valley (RMS, LAR1) sites in all groups. In fact, U began increasing at all of the other sites while U at BLU was still decreasing from its nocturnal maxima. The increase in U to midday maxima at BLU also clearly trailed that of other sites in the valley for THRM and SYNW, both on the sidewall and in the upper valley. The timing was much closer for SYNX (Fig. 4).

While some individual cases included in each group might not have followed typical transition sequences, on average they certainly did so. The averages for each group show the morning transition in wind speed at MID/LAR2 and in the upper valley beginning an hour or more earlier than at BLU (Figs. 2–4). Similarly, the beginning of morning changes in wind direction at BLU trailed other sites shown, on average, except for RMS. It is conjectured that the delay at BLU reflects, at least in part, the effects of the early morning sun on the valley sidewall and the TAF. The differences in the timing of the completion of the wind direction rotation were mostly small between sites, except for MID. While the daytime character of the sensible heat fluxes varied between groups, there was little appreciable difference in the timing of the transition from negative to positive sensible heat flux between sites. The change in sign was approximately coincident with or preceded changes in the other criteria.

For THRM, the wind directions at the upper valley sites began to shift to downvalley before, but more slowly than, the lower valley sites ahead of evening transition (especially BLU; Fig. 2).

Figures 5 and 6 show wind speed and direction data for the GAP and INV subpopulations of THRM, respectively. Ten-minute average wind speed and direction are shown for four sites in the upper valley

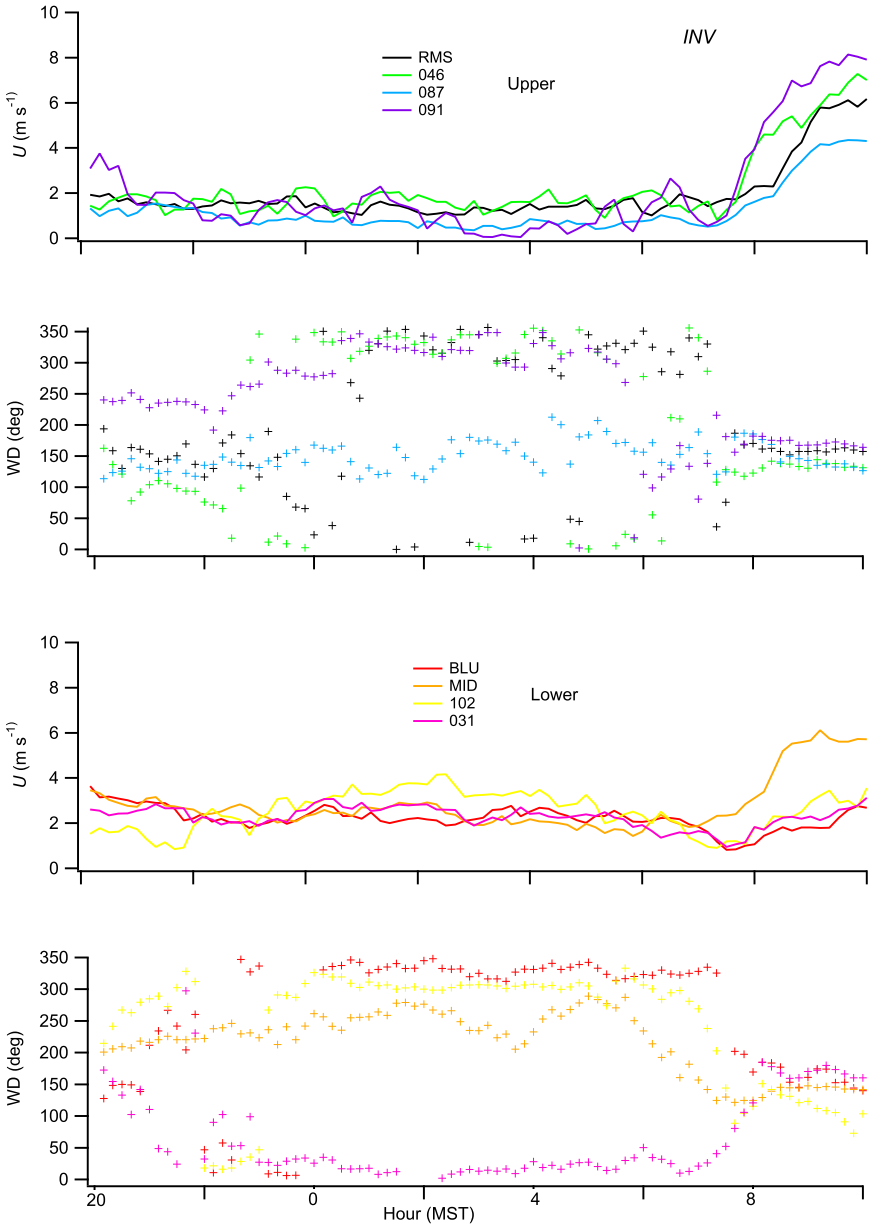

FIG. 6. As in Fig. 5, but for all days in THRM INV.

(RMS, 046, 087, 091) and four sites in the lower valley (BLU, MID, 102, 031). Figure 5, the GAP condition, shows that U in the upper valley was much less than U in the lower valley. Furthermore, while MID on the lower valley sidewall had larger U than the upper valley, it was much lower than U at other sites at lower elevation in the lower valley. The U began to increase in the upper valley during morning transition while it was still declining in the lower valley. However, the wind direction shift during morning transition was larger and more rapid at the lower valley sites than the upper valley sites. Figure 6, the INV condition, shows that U was similarly small at all sites in the upper and lower valley until about 0700–0800 h. During that time U in the upper valley began to increase to their daytime maxima while U in the lower valley remained small, even decreasing. Again, MID on the valley sidewall was an exception as U there began to increase in the same way as in the upper valley. Wind directions began to switch slightly earlier, about 20 min, at MID and the upper valley sites than the remaining lower valley sites, consistent with TAF considerations. These data suggest that the THRM GAP condition promoted an earlier transition in the morning to upvalley winds in the lower valley relative to the upper valley.

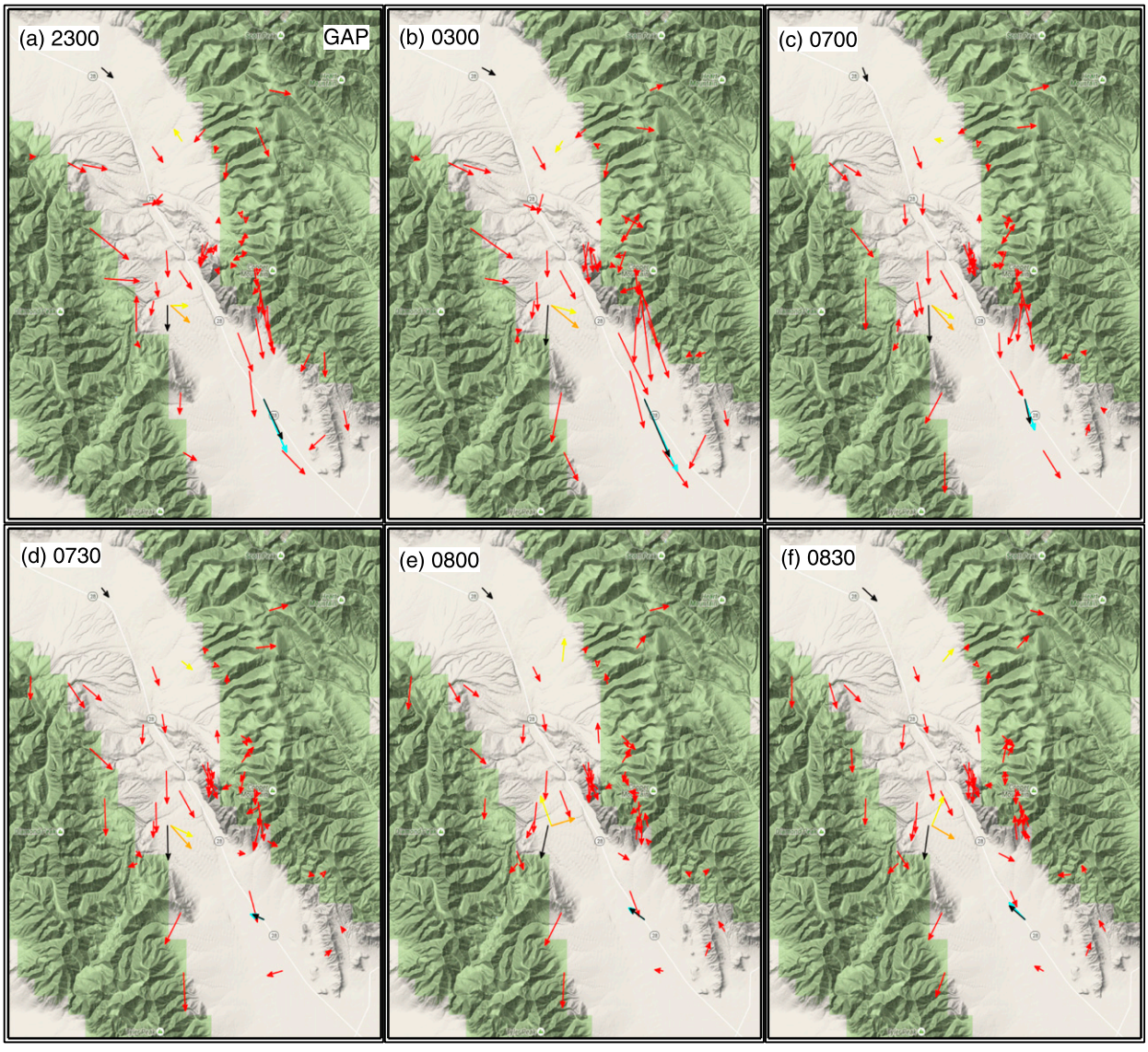

FIG. 7. Ten-minute average wind vector maps for GAP example at (a) 2300, (b) 0300, (c) 0700, (d) 0730, (e) 0800, and (f) 0830 h MST on 21–22 Jul showing FSL (red, 3 m), ARLFRD (black, 3.2 m; cyan, 15 m), and LAR (yellow, 3 m; orange, 8 m) anemometer sites. Heights given in AGL.

The temporal evolution of a GAP case is shown in Fig. 7. At 2300 and 0300 h light winds were present in the upper valley and there were strong winds along the axis of the lower valley at the lowest elevation. At 0700 h wind speeds in the lower valley began to decline but wind directions were still northwesterly in both the upper and low valleys. At 0730, 0800, and 0830 h, wind speeds dropped sharply and wind directions began to shift in the lower valley while there was little change in the upper valley. Figure 8 shows the synoptic weather pattern over a 4-day GAP-criteria period that included this case. BCV lay within a broad high pressure ridge.

The temporal evolution of an INV case is shown in Fig. 9. At 2300 and 0300 h winds were very light and variable in both the upper and lower valleys. By 0700 h wind directions in the upper valley shifted to upvalley and wind speeds increased slightly while winds in the lower valley remained very light and variable. That pattern persists through the remaining time steps shown although wind directions in the lower valley are beginning to organize to upvalley by 0900 h. Figure 10 shows the synoptic weather pattern over a 4-day INV-criteria period that included this case. BCV lay near the boundary between a large ridge in the central United States and a large trough to the northwest. While U did not reach threshold levels for SYNW at SMC, Fig. 10 suggests there was synoptic influence in these cases.

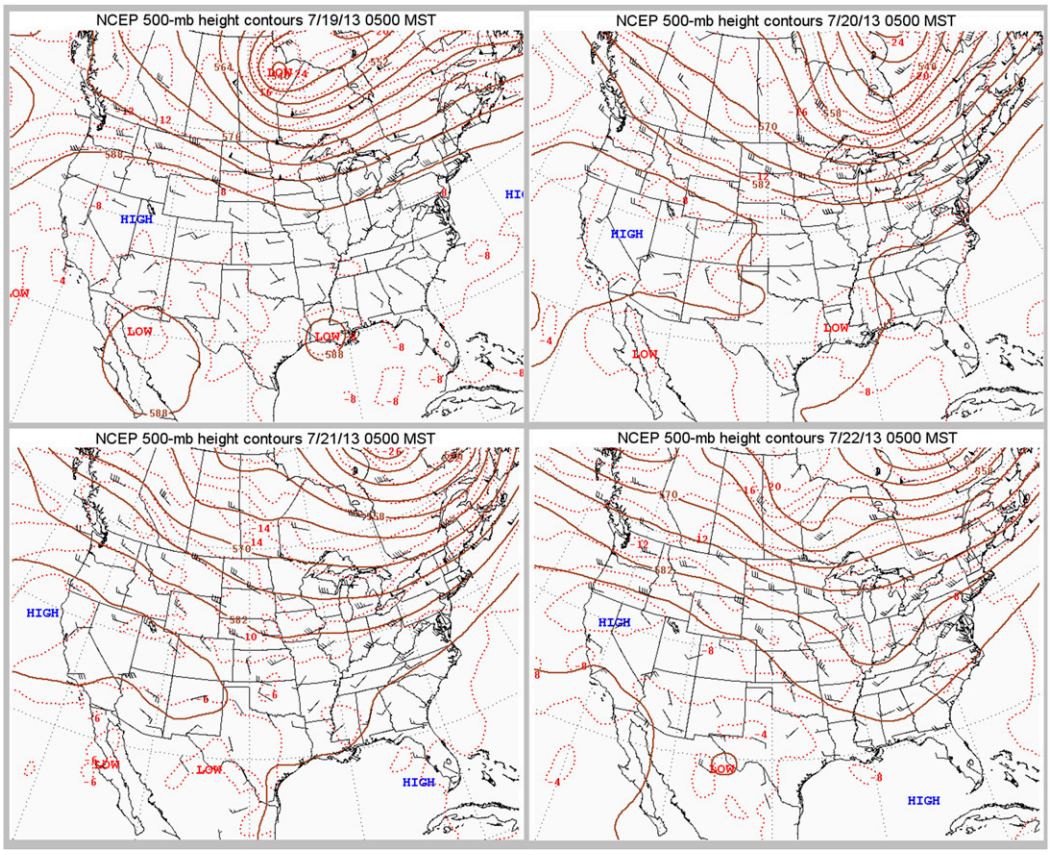

FIG. 8. 500-mb height contours (solid lines) showing the synoptic pattern for the 4-day GAP-criteria period that encompasses the example shown in Fig. 7. All times are 0500 h MST.

b. *Effects of synoptic factors*

The effects of synoptic factors at BLU during nighttime is a decrease in the strength of U as demonstrated by the significantly lower mean nocturnal wind speeds for the SYNW and SYNX groups compared to THRM (Figs. 2–4). It was noted in section 2c that of the 44 THRM days, 23 were GAP and 8 were INV. This suggests that GAP conditions have an affinity for THRM days in summertime in BCV since they developed on about half of such days. The SYNW and SYNX groups were also examined for when the GAP and INV criteria at BLU were satisfied. The results shown in Table 2 suggest that GAP-criteria conditions were about twice as likely to occur in THRM conditions as in SYNW and SYNX conditions whereas the INV condition was more likely to be associated with SYNW. A comparison of Figs. 8 and 10 also suggests that THRM INV was more influenced by synoptic factors than THRM GAP.

TABLE 2. Number of days satisfying GAP and INV criteria within each group.

Group	Total days	GAP days	INV days
THRM	44	23	8
SYNW	16	4	8
SYNX	26	6	4

The inclusion of GAP and INV in all three groups might be considered an unexpected result. However, strong surface heating and cooling were usually prominent factors for several hours each day for all groups in the arid environment of BCV. Days that featured sustained periods with higher afternoon wind speeds linked to synoptic forcing could also still be significantly affected by strong daytime surface heating and nighttime radiative cooling. Days affected by thunderstorms and cloudiness were also commonly affected for significant periods of time by strong surface heating and cooling. In particular, it will be shown below, that there were some similarities between the thermal evolution of THRM GAP cases and THRM/other cases as well as some SYNW and SYNX GAP cases.

c. *Stability measurements and TAF estimates*

Figure 11 shows results for N classified into the THRM, SYNW, and SYNX groups and then by GAP, INV, and "other" cases within each group for which

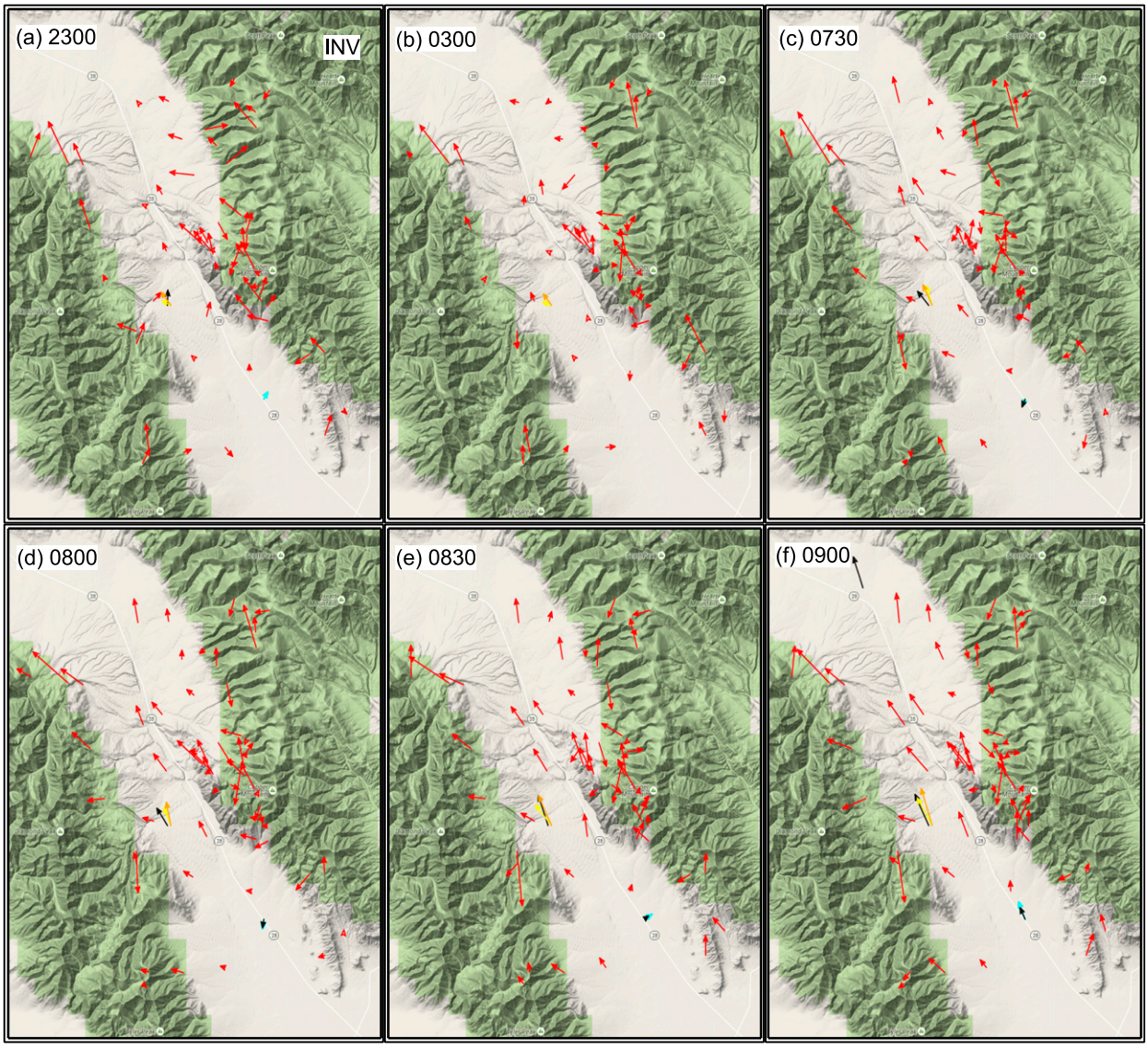

FIG. 9. Ten-minute average wind vector maps for INV example at (a) 2300, (b) 0300, (c) 0730, (d) 0800, (e) 0830, and (f) 0900 h MST on 27–28 Aug. Site information as in Fig. 7.

data is available. Other represents those cases where neither the GAP nor INV criteria were satisfied at BLU. The GAP cases characteristically show *N* increasing at both BLU and LAR1 during the evening before *N* decreased overnight at BLU creating a large difference. This drop is coincident with the onset of gap flows downwind of the constriction. For the SYNW GAP case, this occurred later at night. All of the GAP results shown here were associated with ridging or zonal flow. Nevertheless, the SYNX and SYNW results suggest that GAP-criteria conditions at BLU could develop in situations where there was some evidence of synoptic influences.

THRM/other histories resemble those of THRM GAP and SYNX GAP but the difference in *N* between LAR1 and BLU is somewhat less and probably prevented development of GAP-criteria conditions at BLU. The INV cases are characterized by *N* at BLU and LAR1 being roughly equal most of the night with matching trends. SYNW is associated with the largest magnitude *N*. For SYNW and SYNX other, the magnitude of *N* at BLU appears to have been insufficient to create INV-criteria conditions while the decrease in *N* that is associated with GAP-criteria conditions at BLU did not occur.

The vertical cross-sectional form of the TAF calculation described in Whiteman (1990) was used to find TAF for representative cross sections of the upper and lower valleys. The TAF for the upper and lower valleys, relative

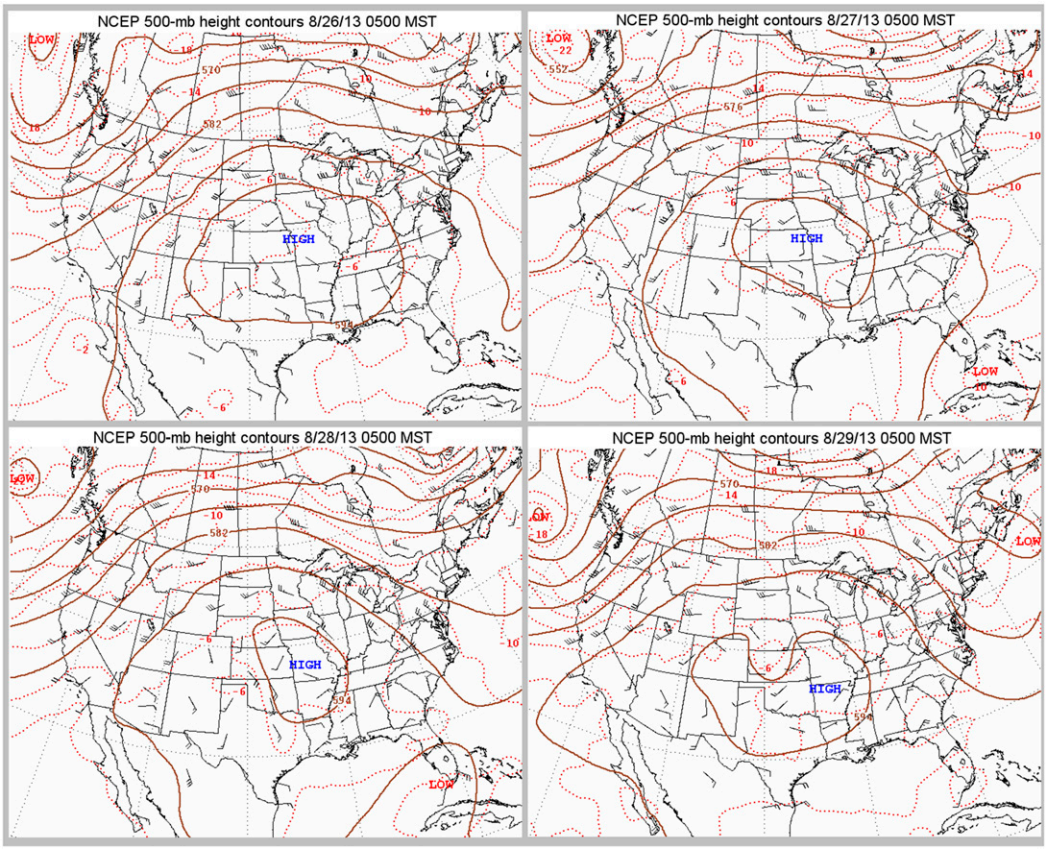

FIG. 10. As in Fig 8, but for the 4-day INV-criteria period that encompasses the example shown in Fig. 9.

to the plain, were estimated to be 2.34 and 2.96, respectively. The ratio of the cross-sectional areas below ridgeline of the lower valley divided by the upper valley is 1.15.

d. Sodars

Figure 12 shows the evolution of the sodar wind profiles at BLU and MID with emphasis on the period from near the start of evening transition to near the start of morning transition for THRM GAP. There was a well-defined jet maximum at about 60–70 m AGL at BLU between 0000 and 0400 h with mean U in excess of 10 m s^{-1} and north-northwest wind directions. The jet profile loses definition after 0500 h. In contrast, while local topography probably has a greater influence at MID than BLU, there was no evidence of jetlike profiles at MID up to 200 m AGL. It was seen previously (Fig. 5) that U at the elevated MID sidewall site were less than U at lower elevation sites in the lower valley. In combination with the sodar observations, this suggests the existence of a low-level jet with a maximum at a lower height centered along the axis of the lower valley. The evening transition was marked by a wind direction shift from the daytime azimuth of about 170° to a nighttime azimuth of about 330°.

Figure 13 shows sodar wind profiles at BLU and MID for THRM INV. Jetlike profiles were absent at both sites at any time. Nocturnal wind speeds at BLU were very light, much less than for GAP, and wind direction profiles were highly variable. Nocturnal wind speeds at MID were slightly higher with wind directions dominantly south-southeast. The significance of the contrasts between Figs. 12 and 13 will be discussed further in section 4.

e. Radar wind profiler

The half-hour records from the radar wind profiler at BLU for the THRM GAP and INV conditions were averaged to 1 h for the time periods shown in Fig. 14. The most striking feature is the inverted nocturnal wind speed profiles for GAP. The wind speeds decreased to a local minimum at about 1 km AGL at 0000 h with the minimum gradually shifting downward through the night. The wind directions were northwesterly below this minimum and rapidly rotated counterclockwise to southwesterly above the minimum and coupled with flows above the valley. In contrast, there was an absence of local minimum wind speeds in the INV profiles. While wind directions in INV were similar to GAP aloft

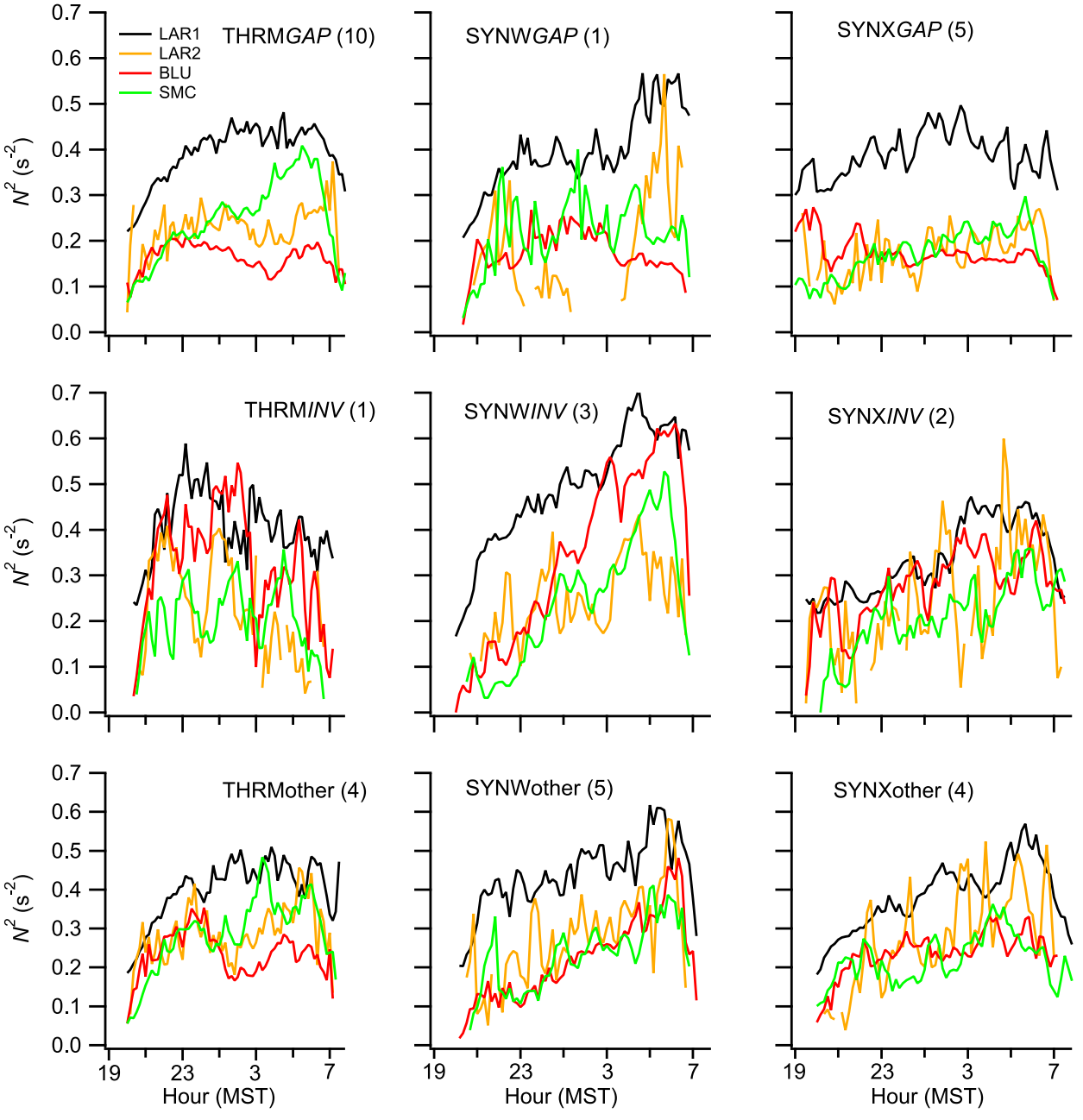

FIG. 11. Average squared Brunt–Väisälä frequencies (N^2) at LAR1, LAR2, BLU, and SMC by synoptic group (THRM, SYNW, SYNX), and GAP, INV, or other (non-GAP, non-INV) classification. The number in parentheses represents the number of cases included in the corresponding average.

(southwesterly), the INV wind directions were also from south and southwest near the surface.

f. Gap wind dimensional analysis

An attempt was made at using a dimensional analysis to model U downwind of the constriction (U_2) using the available measurements including N, U upwind of the constriction at LAR1 (U_1), and the cross-sectional areas below ridgeline of the upper and lower valleys (X_1 and X_2, respectively):

$$U_2 = U_1(X_2/X_1)(N_1/N_2)^z, \tag{1}$$

where z is a fitting parameter. The X_2/X_1 factor represents the effects of the topographic amplification factor and the N_1/N_2 factor represents the effects of stability conditions.

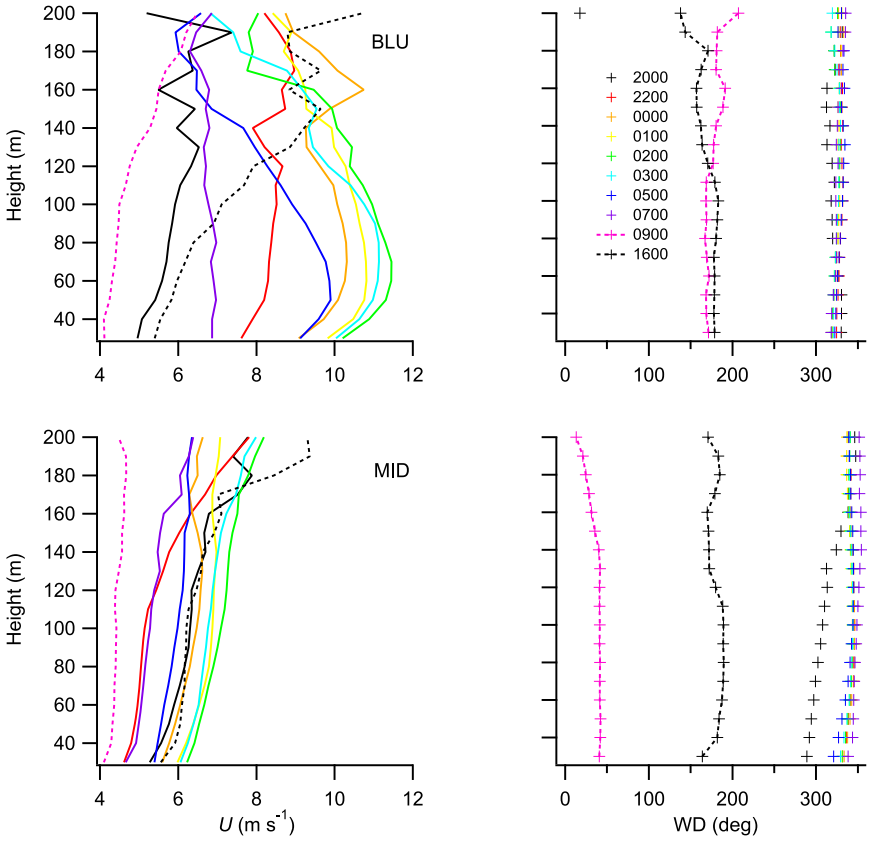

FIG. 12. Average hourly vertical profiles of sodar (left) wind speed and (right) direction for THRM GAP at BLU and MID with emphasis between evening and morning transitions. The start times (MST) for each hour interval are shown in the legend.

The least squares best fit results, given by $z = 1.07$ for THRM GAP at BLU, are shown in Fig. 15a. There is an underprediction bias owing to the influence of some outlier data on the best fit. Figure 15b shows the results for THRM GAP at BLU using $z = 1.3$ and the fit for the bulk of the data is much better. Figure 15c shows the results for THRM GAP at LAR2 using $z = 1.07$ and there is generally a good fit.

Figure 16 shows the results of this method applied to all of the other data subsets at BLU and LAR2 for $z = 1.07$. This hints that the relationship intended to model THRM GAP conditions might also apply to other conditions, excluding INV cases. The analysis suggests that this general approach might provide some insight into the parameterization of gap flows.

The limitations on this analysis should be noted. It relies on a limited record from the lone vertical profile site upwind of the constriction. Furthermore, the LAR1 site was on the sloped eastern the flank of the valley, not near the valley axis like BLU in the lower valley. The analysis is also based on 10-min records with a large spatial separation so the comparison can only be considered in an aggregated sense.

g. *Downwind persistence of gap flows*

Gap flows had a strong influence at SMC, well downstream from the BCV. Figure 17 shows wind roses for THRM GAP days and for the remaining THRM days from 0000 to 0500 h at the 15- and 45-m levels. The GAP days were dominated by north-northwesterly winds from BCV at both levels whereas there was a greater weighting toward the more northeasterly winds of the SRP nocturnal flow regime for the non-GAP days, especially at 45 m. The GAP cases also had a much higher percentage of higher wind speeds. The wind rose data indicate that the BCV exit flow in GAP conditions often persisted at least as far as SMC and was often more than 45 m in depth.

4. Discussion

Table 3 summarizes some of the key features and distinctions between GAP and INV.

Following evening transition in GAP, winds in the lower valley shifted quickly from up- to downvalley, accompanied by an increase in wind speed. Winds in the

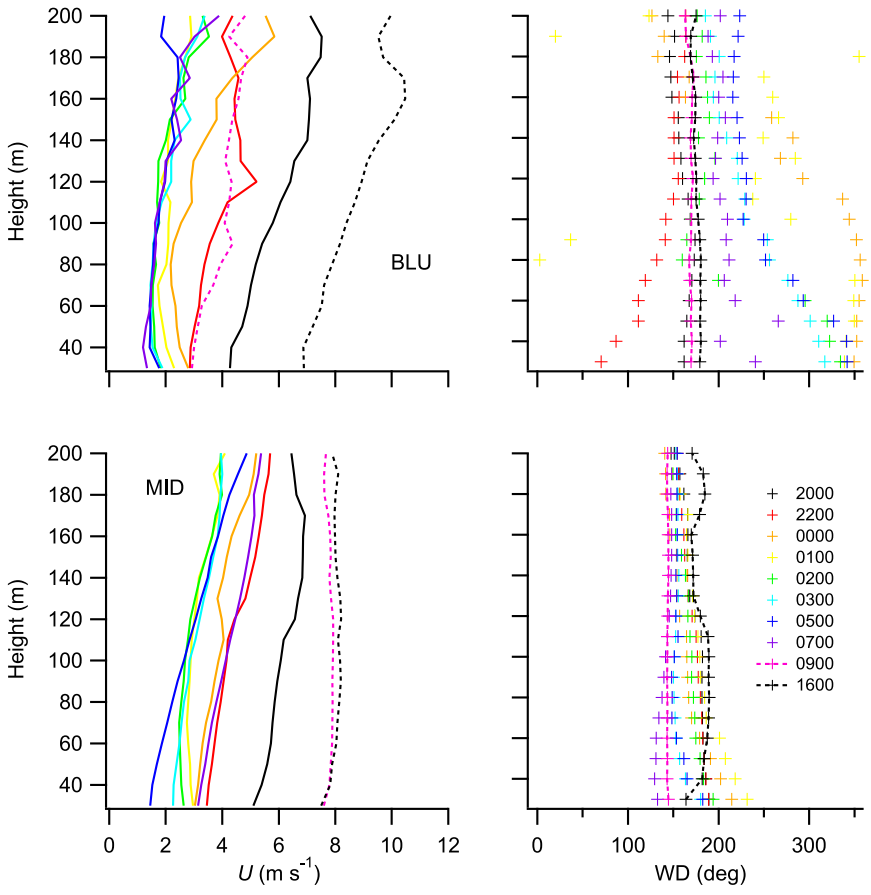

FIG. 13. As in Fig. 12, but for THRM INV.

upper valley upwind of the constriction were very light and remained that way throughout the night. The turning in wind direction downwind of the constriction was more rapid along the valley bottom (BLU) than along the flanks of the valley (MID) (Figs. 2 and 5). Beginning about 2300 h, about 3–4 h after transition, the cold air pool in the upper valley reached a critical point and spilled over and through the midvalley constriction and accelerated into the lower valley. High downvalley winds persisted downwind of the constriction in the lower valley from 2300 h until after sunrise (~0700–0800 h), tending to gradually decrease following maxima usually occurring between 0100 and 0400 h.

GAP was best developed with higher U along the bottom of the lower valley (BLU) and weaker on the valley sidewall (MID). Jetlike profiles were present along the valley axis with wind speed maxima of 10–12 m s^{-1} at 60–70 m AGL but absent along the valley sidewall (Fig. 12). The overall depth of the layer up to the local wind speed minimum was about 1 km at midnight (~depth of valley) then decreasing to about 0.5 km near transition. Zängl (2004) reports low-level jets in the exit region in simulations for an Alpine valley with wind speed maxima of 12 m s^{-1} at 200 m AGL.

While GAP criteria were not met for all THRM cases, nocturnal north-northwest winds at BLU still dominated THRM (Fig. 2). That is, moderate to strong downvalley winds routinely developed at BLU in THRM even if they did not always reach GAP criteria.

Some of the key distinctions between GAP and INV are tied to stability conditions in the BCV. Figure 11 suggests that GAP conditions were most commonly triggered when the observed differences in N (LAR1 versus BLU) were near a maximum, most commonly in the late evening. The triggering of GAP conditions in the lower valley was accompanied by a drop in N. In contrast, N increased through the night for INV in both the upper and lower valleys. The decrease in N for GAP in the lower valley (BLU) is presumed to be related to greater mixing accompanying the increase in U.

The persistence of nocturnal southerly winds in the lower valley appears to be the factor in common in the development of INV conditions and the suppression of GAP conditions. The persistence of these southerly flows can be linked to synoptic forcing. INV criteria had their strongest association with the high daytime U SYNW group (section 3b). High daytime U at SMC were

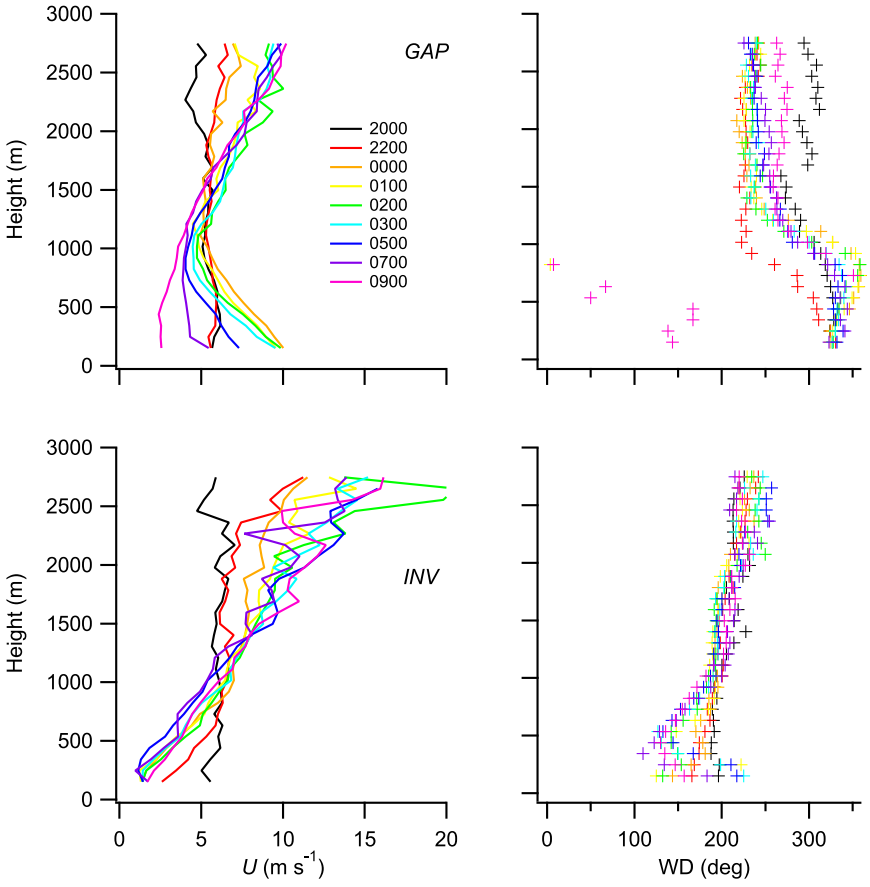

FIG. 14. Average hourly vertical profiles of radar profiler (left) wind speed and (right) direction for GAP and INV at BLU with emphasis between evening and morning transitions. The start times (MST) for each hour interval are shown in the legend.

predominantly from the southwest and any persistence of them into the nighttime would act to interfere with the thermal regime requisite for GAP development and suppress downvalley outflows from BCV. SYNW showed stronger persistence of south-southwest winds through evening transition at sites in the lower valley than THRM (cf. Figs. 2 and 3). Comparisons between GAP and INV (Figs. 5 and 6; Figs. 12 and 13; Fig. 14) show a much greater prevalence for southerly winds in the lower valley at night for INV than GAP, especially at MID and above the surface. Figures 2–4 show nocturnal wind direction rotation to downvalley downwind of the constriction was the norm near the surface. However, Fig. 13 suggests this was limited to a shallow layer up to about 100 m along the axis of the valley for INV conditions with synoptically forced southerly flows. The southerly nocturnal flows in the lower valley during INV would be consistent with the synoptic pattern shown in Fig. 10.

It is emphasized that GAP-criteria conditions in BCV did not appear to be the exclusive domain of quiescent, nonsynoptic conditions. Fair weather conditions certainly promoted their development but they also developed in situations featuring synoptic influences. This was mostly the case when cloudiness, rain, and thunderstorm activity ± high U were potential factors (SYNX). If the timing of these weather events was such that the requisite precursor stability regime was still able to establish itself in the upper and lower valleys by the time of evening transition, then GAP conditions could develop. Similar can be said for SYNW. If synoptic forcing was weak enough to allow southerly daytime winds to subside sufficiently by evening transition, then GAP conditions could develop. The key features appear to be the stability regime and strength of synoptically driven southerly flow at evening transition.

The distinctions between GAP and INV had consequences on morning transition. Figure 5 (THRM GAP) shows that wind directions in the lower valley were shifting rapidly from north-northwest (downvalley) to southeast (upvalley) between 0800 and 0900 h. In the upper valley, the wind direction at sites there changed very slowly and remained out of the

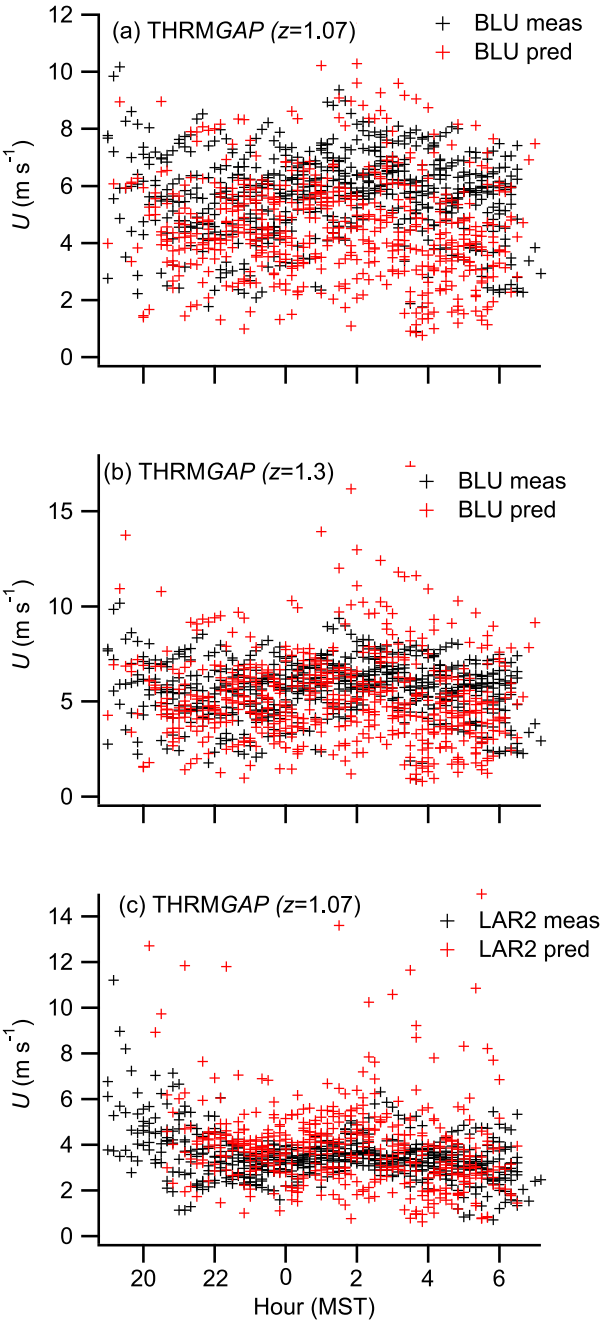

FIG. 15. Predicted vs measured wind speeds downwind of the constriction based upon dimensional analysis [Eq. (1)] for the available THRM GAP cases for (a) BLU with $z = 1.07$, (b) BLU with $z = 1.3$, and (c) LAR2 with $z = 1.07$.

northwest. Wind speeds at the lower valley sites hit their minimum and began to increase after 0900 h while the upper valley sites showed little change. Thus the morning transition in the lower valley, on average, occurred ahead of the upper valley for THRM GAP (also see Fig. 7). It is conjectured that the earlier shift to upvalley winds in the lower valley for THRM GAP was due to the enhanced nighttime mixing and weakening of the inversion there.

In contrast, THRM INV (Fig. 6) shows that wind speeds in the upper valley began to increase sharply by 0800 h while U in the lower valley showed little variation except at MID. The shift from nocturnal wind directions to southerly (upvalley) in the upper valley was complete before 0800 h while this occurred about one-half hour later in the lower valley (also see Fig. 9).

It is hypothesized that the delay in morning transition at BLU and other lower valley sites (excepting the western sidewall), relative to sites in the upper valley, is an expression of the TAF. This would apply for INV as well as more generally to all non-GAP conditions. Mountain valley inversions are known to usually develop to full valley depth (Whiteman 1990). The conjecture is that the persistence of a relatively stronger inversion in the lower valley inhibited morning transition, delaying it relative to the western sidewall (MID, LAR2) and the upper valley. That is, it took longer to heat a deeper pool of cold air to break the inversion in the lower valley than it did to heat a thinner layer of air above the inversion in the lower valley, or the shallower pool of cold air in the upper valley. Steinacker (1984) and Whiteman (1990) have discussed this stability effect. Whiteman (1982) has described the mechanisms by which deep valley inversions are broken. Thus the morning transition in the upper valley occurred ahead of the lower valley for non-GAP conditions. In contrast, the weakly stable boundary layer in the lower valley associated with GAP promoted a more rapid morning transition there relative to the upper valley.

Future numerical modeling work could confirm our hypotheses and perhaps facilitate a better understanding of the valley-scale gap flow events suggested by our measurements. It would be worthwhile to investigate whether large-eddy simulations (LES) are able to capture the thermal and mechanical dynamics associated with these flow events. Others have successfully used LES to investigate similar flow dynamics and thermal circulations in steep alpine valleys (e.g., Weigel et al. 2006). The flow dynamics observed during the BCV field campaign are a manifestation of flows associated with several different scales of motion (e.g., slope flows, valley flows, and synoptic-scale flows) superimposed on one another. While the basic physics driving the dynamics at the various scales is fairly well understood for idealized cases (e.g., Whiteman 2000), the effects of heterogeneity of real terrain and the interaction of these flows at various scales are not. Numerical modeling applied to real terrain cases, such as the BCV, could help bridge this gap.

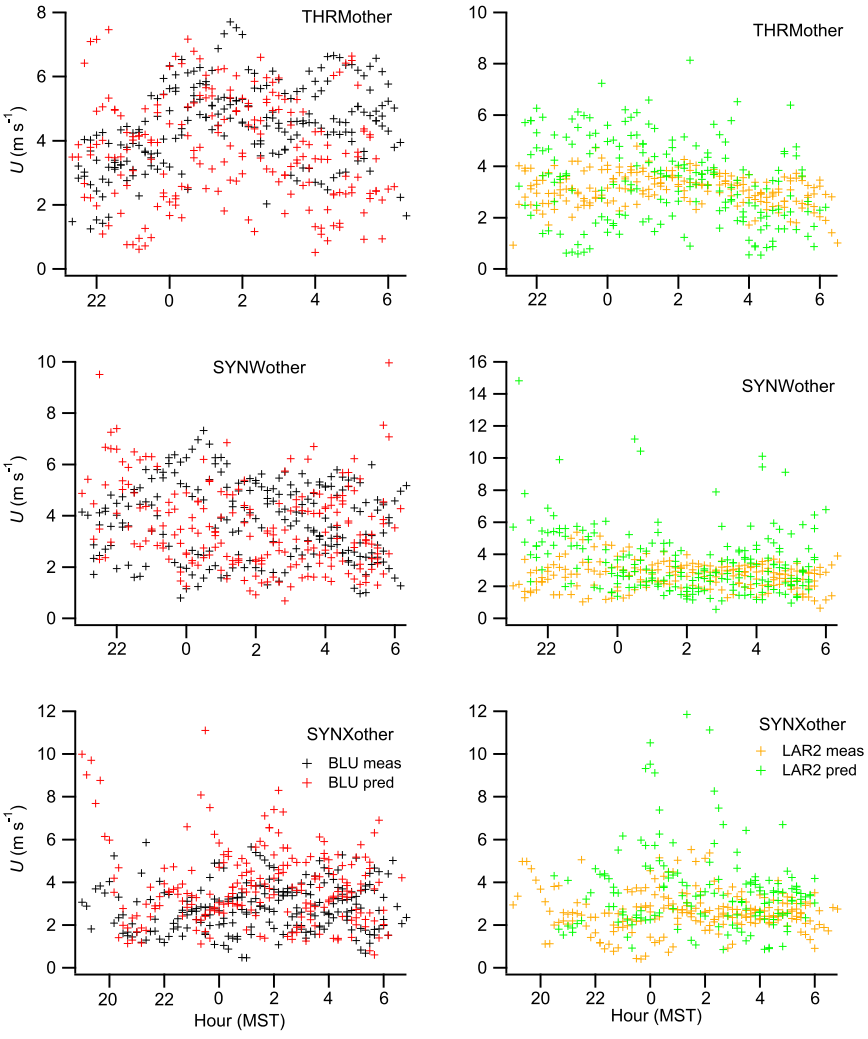

FIG. 16. Predicted vs measured wind speeds downwind of the constriction based upon dimensional analysis [Eq. (1)] for the available other cases (non-GAP and non-INV) by synoptic group at BLU and LAR2.

This will not be fully developed here but it is interesting to note that the nighttime wind speeds at the HOW and ARC NOAA/INL Mesonet stations are often strong from the northwest, similar to BLU. These two stations lie near where two adjacent mountain valleys to the west of BCV open out onto the SRP. However, in general, valley outflows there are not quite as strong or consistent as those observed at BLU and it is unknown if nocturnal downvalley exit jets occur similar to BCV, are more weakly developed, or are absent. This could be a matter of these stations being positioned further outside of their respective valleys than BLU and are more influenced by winds on the SRP. It might also be due to different valley configurations. For example, HOW sits near the mouth of the Little Lost River Valley, which has more kinks in its course but lacks a constriction like that of BCV.

5. Conclusions

A topographic obstruction midway in BCV separates it into an upper and lower valley with two different flow regimes. The results shown here describe some of the airflow differences between the upper and lower valleys. The analysis highlighted the strong evidence for the existence of gap flows in BCV in certain conditions. In general, the frequency and strength of gap flows in the BCV setting appears to be linked to the minimization of synoptic forcing. Realization of the GAP criteria and strong gap flows was most closely associated with the THRM group. However, GAP-criteria conditions were

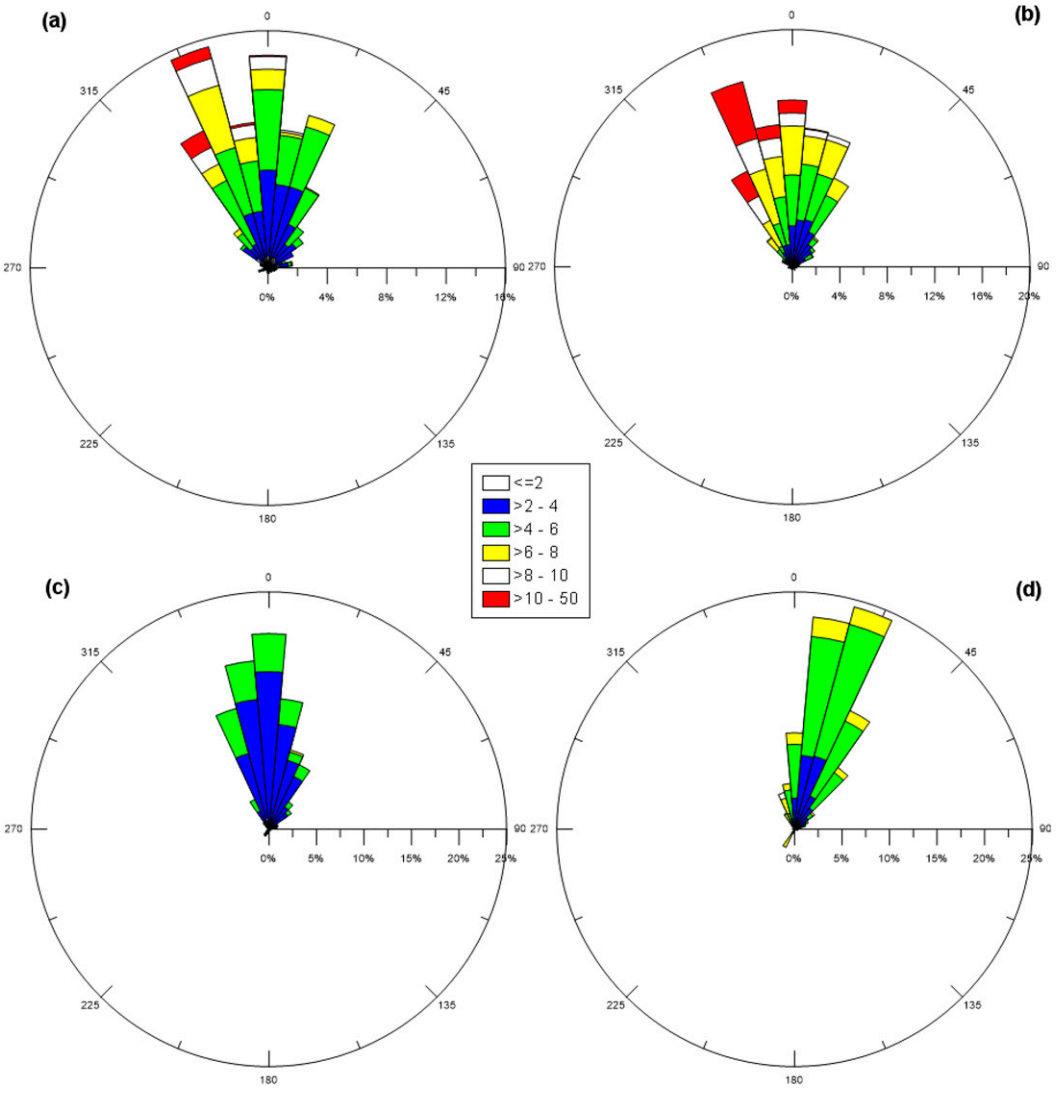

FIG. 17. Wind roses (m s^{-1}) from SMC for THRM (a),(b) GAP and (c),(d) non-GAP cases at the 15- and 45-m levels, respectively, using 5-min-average data showing the effects of BCV GAP category flows out on the SRP between 0000 and 0500 h MST.

sometimes realized in situations with synoptic influences if the necessary stability conditions were able to develop and any synoptically forced southerly winds at the time of transition were minimal. The presumed effects of the TAF affected the timing and sequence of developments between the upper valley, lower valley, and lower valley sidewall during morning transition. For all three groups the morning transition in the upper valley and western sidewall proceeded, on average, slightly ahead of the lower valley. The exception to this was when strong

TABLE 3. Summary of key observations for GAP and INV.

GAP	INV
• High nighttime *U* at BLU (Figs. 2 and 5)	• Low nighttime *U* at BLU (Fig. 6)
• Increasing *N* early in upper and lower valley then sharp decrease in lower valley (Fig. 11)	• High *N* that increases through the night in both the upper and lower valleys (Fig. 11)
• Strongest association with THRM (Table 2)	• Strongest association with SYNW (Table 2)
• Distinct nocturnal flow reversal in lower valley from southerly to north-northwesterly (Figs. 2 and 12)	• No well-defined nocturnal flow reversal in lower valley; persistence of southerly flows, especially at MID (Figs. 6 and 13)
• Transition in lower valley ahead of upper valley (Fig. 5)	• Transition in upper valley ahead of lower valley (Fig. 6)

nocturnal gap flows in the lower valley largely mixed out the inversion there allowing for a more rapid morning transition than in the upper valley.

The data and analysis provide guidance about potential geographic and meteorological conditions that could significantly influence wildland fire spread and intensity.

The limitations imposed by the available measurements leave many unanswered questions. Additional temperature profile data in both the upper and lower valleys would have been very helpful in fully discerning the role of stability conditions and defining the circumstances that trigger the development of gap flows and how strong and persistent they become.

Acknowledgments. We thank Dan Jimenez, Cyle Wold, and Paul Sopko for their assistance with the FSL deployment. We also thank Shane Beard and Tom Strong from ARLFRD for their work in maintaining the ARLFRD and LAR instrumentation during the field study. Funding for this work was provided in part by NOAA and the National Fire Plan and the Joint Fire Science Program (Project 10-1-07-16). The WSU participation of this work was partly supported by NSF AGS under Grant 1419614.

REFERENCES

Aubinet, M., and Coauthors, 2000: Estimates of the annual net carbon and water exchange of forests: The EUROFLUX methodology. *Adv. Ecol. Res.*, **30**, 113–175, doi:10.1016/S0065-2504(08)60018-5.

Banta, R. M., L. D. Olivier, W. D. Neff, D. H. Levinson, and D. Ruffieux, 1995: Influence of canyon-induced flows on flow and dispersion over adjacent plains. *Theor. Appl. Climatol.*, **52**, 27–41, doi:10.1007/BF00865505.

Bendall, A. A., 1982: Low-level flow through the Strait of Gibraltar. *Meteor. Mag.*, **111**, 149–153.

Butler, B. W., and Coauthors, 2015: High-resolution observations of the near-surface wind field over an isolated mountain and in a steep river canyon. *Atmos. Chem. Phys.*, **15**, 3785–3801, doi:10.5194/acp-15-3785-2015.

Chrust, M. F., C. D. Whiteman, and S. W. Hoch, 2013: Observations of thermally driven wind jets at the exit of Weber Canyon, Utah. *J. Appl. Meteor. Climatol.*, **52**, 1187–1200, doi:10.1175/JAMC-D-12-0221.1.

Clawson, K. L., R. M. Eckman, N. F. Hukari, J. D. Rich, and N. R. Ricks, 2007: Climatography of the Idaho National Laboratory. 3rd ed. NOAA Tech. Memo. OAR ARL-259, Air Resources Laboratory, 254 pp. [Available online at http://www.arl.noaa.gov/documents/reports/arl-259.pdf.]

Colle, B. A., and C. F. Mass, 2000: High resolution observations and numerical simulations of easterly gap flow through the Strait of Juan de Fuca on 9–10 December 1995. *Mon. Wea. Rev.*, **128**, 2398–2422, doi:10.1175/1520-0493(2000)128<2398:HROANS>2.0.CO;2.

Darby, L. S., K. J. Allwine, and R. M. Banta, 2006: Nocturnal low-level jet in a mountain basin complex. Part II: Transport and diffusion of tracer under stable conditions. *J. Appl. Meteor. Climatol.*, **45**, 740–753, doi:10.1175/JAM2367.1.

Dorman, C. E., R. C. Beardsley, and R. Limeburner, 1995: Winds in the Strait of Gibraltar. *Quart. J. Roy. Meteor. Soc.*, **121**, 1903–1921, doi:10.1002/qj.49712152807.

Fernando, H. J. S., and Coauthors, 2016: The MATERHORN: Unraveling the intricacies of mountain weather. *Bull. Amer. Meteor. Soc.*, **96**, 1945–1967, doi:10.1175/BAMS-D-13-00131.1.

Flannigan, M. D., M. A. Karwchuk, W. J. de Groot, B. M. Wotton, and L. M. Gowman, 2009: Implications of changing climate for global wildland fire. *Int. J. Wildland Fire*, **18**, 483–507, doi:10.1071/WF08187.

Forthofer, J. M., B. W. Butler, C. W. McHugh, M. A. Finney, L. S. Bradshaw, R. D. Stratton, K. S. Shannon, and N. S. Wagenbrenner, 2014: A comparison of three approaches for simulating fine-scale surface winds in support of wildland fire management. Part II. An exploratory study of the effect of simulated winds on fire growth simulations. *Int. J. Wildland Fire*, **23**, 982–994, doi:10.1071/WF12090.

Liu, M., D. L. Westphal, T. R. Holt, and Q. Xu, 2000: Numerical simulation of a low-level jet over complex terrain in southern Iran. *Mon. Wea. Rev.*, **128**, 1309–1327, doi:10.1175/1520-0493(2000)128<1309:NSOALL>2.0.CO;2.

Mayr, G. J., and Coauthors, 2004: Gap flow measurements during the Mesoscale Alpine Programme. *Meteor. Atmos. Phys.*, **86**, 99–119, doi:10.1007/s00703-003-0022-2.

——, and Coauthors, 2007: Gap flows: Results from the mesoscale Alpine programme. *Quart. J. Roy. Meteor. Soc.*, **133**, 881–896, doi:10.1002/qj.66.

Muller, H., R. Reiter, and R. Sladkovic, 1984: Die vertikale windstruktur beim Merkur-Schwerpunkt "Tagesperiodische Windsysteme" aufgrund von aerologischen Messungen im Inntal und im Rosenheimer Becken (On the vertical wind structure of the diurnal wind system within the Inn Valley and the adjacent plain: Results of aerological soundings during the field experiment Merkur). *Arch. Meteor. Geophys. Bioklimatol.*, **33B**, 359–372, doi:10.1007/BF02274002.

Overland, J. E., and B. A. Walter Jr., 1981: Gap winds in the Strait of Juan de Fuca. *Mon. Wea. Rev.*, **109**, 2221–2233, doi:10.1175/1520-0493(1981)109<2221:GWITSO>2.0.CO;2.

Pamperin, H., and G. Stilke, 1985: Nachtliche grenzschicht und LLJ im alpenvorland nahe dem Inntalausgang (Nocturnal boundary layer and low-level jet near the Inn Valley exit). *Meteor. Rundsch.*, **38**, 145–156.

Rampanelli, G., D. Zardi, and R. Rotunno, 2004: Mechanisms of up-valley winds. *J. Atmos. Sci.*, **61**, 3097–3111, doi:10.1175/JAS-3354.1.

Russell, E. S., H. Liu, Z. Gao, D. Finn, and B. Lamb, 2015: Impacts of soil heat flux calculation methods on the surface energy balance closure. *Agric. For. Meteor.*, **214–215**, 189–200, doi:10.1016/j.agrformet.2015.08.255.

Schmidli, J., 2013: Daytime heat transfer processes over mountainous terrain. *J. Atmos. Sci.*, **70**, 4041–4066, doi:10.1175/JAS-D-13-083.1.

——, and R. Rotunno, 2012: Influence of the valley surroundings on valley wind dynamics. *J. Atmos. Sci.*, **69**, 561–577, doi:10.1175/JAS-D-11-0129.1.

Sharp, J., and C. F. Mass, 2002: Columbia Gorge gap flow—Insights from observational analysis and ultra-high-resolution simulations. *Bull. Amer. Meteor. Soc.*, **83**, 1757–1762, doi:10.1175/BAMS-83-12-1757.

——, and ——, 2004: Columbia Gorge gap winds: Their climatological influence and synoptic evolution. *Wea. Forecasting*, **19**, 970–992, doi:10.1175/826.1.

Sladkovic, R., and H.-J. Kanter, 1977: Low-level jet in the Bavarian pre-Alpine region. *Arch. Meteor. Geophys. Bioklimatol.*, **25A**, 343–355, doi:10.1007/BF02317994.

Steinacker, R., 1984: Area-height distribution of a valley and its relation to the valley wind. *Contrib. Atmos. Phys.*, **57**, 64–71.

Stewart, J. Q., C. D. Whiteman, W. J. Steenburgh, and X. Bian, 2002: A climatological study of thermally driven wind systems of the U.S. Intermountain West. *Bull. Amer. Meteor. Soc.*, **83**, 699–708, doi:10.1175/1520-0477(2002)083<0699:ACSOTD>2.3.CO;2.

Weigel, A. P., F. K. Chow, M. W. Rotach, R. L. Street, and M. Xue, 2006: High-resolution large-eddy simulations of flow in a steep alpine valley. Part II: Flow structure and heat budgets. *J. Appl. Meteor. Climatol.*, **45**, 87–107, doi:10.1175/JAM2323.1.

Westerling, A. L., H. G. Hidalgo, D. R. Cayan, and T. W. Swetnam, 2006: Warming and earlier spring increase western U.S. forest wildfire activity. *Science*, **313**, 940–943, doi:10.1126/science.1128834.

Whiteman, C. D., 1982: Breakup of temperature inversions in deep mountain valleys: Part I. Observations. *J. Appl. Meteor.*, **21**, 270–289, doi:10.1175/1520-0450(1982)021<0270:BOTIID>2.0.CO;2.

——, 1990: Observations of thermally developed wind systems in mountainous terrain. *Atmospheric Processes over Complex Terrain*, *Meteor. Monogr.*, No. 45, Amer. Meteor. Soc., 5–42.

——, 2000: *Mountain Meteorology: Fundamentals and Applications*. Oxford University Press, 355 pp.

Zängl, G., 2004: A reexamination of the valley wind system in the Alpine Inn Valley with numerical simulations. *Meteor. Atmos. Phys.*, **87**, 241–256, doi:10.1007/s00703-003-0056-5.

Zardi, D., and C. D. Whiteman, 2012: Diurnal mountain wind systems. *Mountain Weather Research and Forecasting: Recent Progress and Current Challenges*, F. K. Chow, F. S. J. DeWekker, and B. Snyder, Eds., Springer, 35–119.